Oxidation-Reduction of $Pb_2Sr_2Ln_{1-x}M_xCu_{3-y}Ag_yO_{8+\delta}$

P. K. Gallagher,* H. M. O'Bryan, R. J. Cava, A. C. W. P. James, D. W. Murphy, W. W. Rhodes, J. J. Krajewski, W. F. Peck, and J. V. Waszczak

AT&T Bell Laboratories, Murray Hill, New Jersey 07974

Received January 3, 1989

The effects of oxygen partial pressure (P_{O_2}) and temperature on the oxygen content, structure, and phase stability of $Pb_2Sr_2YCu_3O_{8+\delta}$, $Pb_2Sr_2GdCu_3O_{8+\delta}$, $Pb_2Sr_2Y_{0.60}Ca_{0.40}Cu_3O_{8+\delta}$, and $Pb_2Sr_2YCu_{2.50}Ag_{0.50}O_{8+\delta}$ are determined. In the range 300–600 °C the compounds with $\delta = 0$ are reversibly oxidized to δ as high as $\approx$1.6. The extent of this reaction depends on the heating rate as well as the temperature and P_{O_2}. The structure changes from orthorhombic to tetragonal, and the unit cell expands on oxidation. The oxygen content in the phase passes through a maximum around 500 °C. Above ~630 °C an irreversible oxidative decomposition occurs depending on the P_{O_2} and nature of the substitutions. The initial decomposition product is a pseudocubic perovskite material, but at still higher oxygen contents a $SrPbO_3$-like perovskite forms. At lower P_{O_2}, where this decomposition does not occur, the original structure undergoes a higher order transformation from orthorhombic to tetragonal symmetry near 750 °C. At temperatures $\gtrsim$850 °C the oxidized products lose O_2 and revert to the original phase and oxygen content. Quenching from above 850 °C or slowly cooling in decreased P_{O_2} can be used to synthesize the orthorhombic structure with $\delta = 0$. The nature and extent of the particular substitutions determine the exact conditions required for various oxygen contents, structures, and phase stability.

Introduction

Cava et al.,[1] have recently reported and Subramanian et al.[2] confirmed a new family of high-T_c oxide superconductors ($T_c \sim 70$ K) having the general formula $Pb_2Sr_2Ln_{1-x}M_xCu_3O_{8+\delta}$, where Ln = La, Y, and rare-earth metals and M = Ca or Sr. Hereafter the abbreviation 2213 will be used to denote this phase. This phase has the orthorhombic structure shown in Figure 1. The basis of the new structure is double planes of corner-shared CuO_5 pyramids, separated by planes of eight-coordinated Ln atoms. These double pyramidal planes sandwich PbO–CuO_δ–PbO planes in an arrangement unique to this family of materials (center of Figure 1, left). In the stoichiometric material (i.e., x and $\delta = 0$), which is not superconducting, it was proposed that the Cu atoms between the PbO layers are monovalent while those in the pyramidal sheets are divalent, leading to an average formal Cu valence of +1.67. As aliovalent ions (M^{2+}) are substituted for Ln^{3+}, it was further postulated that the charge compensation occurs within the pyramidal CuO sheets only, thus raising the average formal valence of these Cu ions beyond +2 and inducing metallic conductivity and superconductivity near $x = 0.5$, $\delta = 0$. It was further proposed that when excess oxygen goes into the structure ($\delta > 0$), it is accommodated in the PbO–CuO_δ–PbO sandwich.

The compounds are unique among hole-doped copper-based high-T_c superconductors in that they must be synthesized under mildly reducing instead of oxidizing conditions, suggesting a very interesting P_{O_2}–temperature phase stability relationship.[1] The host $Pb_2Sr_2LnCu_3O_8$ compounds can be doped with holes by accommodation of excess oxygen, M^{2+}/Ln^{3+} substitution, or a combination of both. Therefore, the detailed understanding of the phase stability under differing conditions is important for further systematic study of these materials. The purpose of this paper is to investigate the changes in oxygen content, phase stability, and structure that occur in several stoichiometric and substituted materials as they are heated in various partial pressures of oxygen, P_{O_2}. The intent is to determine (1) the limits and variability of δ, (2) the range of δ for which the structure in Figure 1 is stable, (3) the changes in lattice parameters as a function of δ, and (4) the decomposition products at both high and low P_{O_2}. The answers to these questions should facilitate the synthesis and provide a basis for further studies of phase equilibria, crystal growth, and properties of these materials as M, x, and δ are varied. To answer these questions, thermogravimetry (TG) and differential thermal analysis (DTA) have been utilized in conjunction with both ambient and high-temperature X-ray diffraction.

Experimental Methods

Materials. Small quantities of $Pb_2Sr_2YCu_3O_8$, $Pb_2Sr_2GdCu_3O_8$, $Pb_2Sr_2Y_{0.75}Ca_{0.25}Cu_3O_8$, $Pb_2Sr_2Y_{0.60}Ca_{0.40}Cu_3O_8$, $Pb_2Sr_2YCu_{2.75}Ag_{0.25}O_8$, and $Pb_2Sr_2YCu_{2.50}Ag_{0.50}O_8$ were prepared as previously described.[1,3]

Thermal Analysis. Perkin-Elmer System 7 high-temperature TG and Du Pont Thermal Analysis 2000 units were used. The gas-flow rate over the samples was 100 mL min^{-1} except for the dilute H_2 (15% H_2–85% N_2), which was 300 mL min^{-1}. An O_2 analyzer at the output of the TG apparatus indicated that the oxygen level was 55–60 ppm in the N_2 flow, and a value of 60 ppm O_2 is subsequently used throughout this paper. The sample pans were Al_2O_3 when forming gas was used and Pt for all other gases. Samples were furnace cooled (slow cooled) unless otherwise noted. A blank run under the same conditions but without a sample was used to correct the measured weights prior to the calculation of stoichiometry. Although this correction is not made in the figures, it has been made prior to the quotation of any numerical value.

The DTA experiments were performed by using a Perkin-Elmer DTA 1700 system. The smaller Al_2O_3 sample crucibles were used, and powdered Al_2O_3 served as the reference material. Either O_2 or N_2 was flowed at 50 mL min^{-1} through the apparatus.

X-ray Diffraction. A Philips automated powder diffractometer was used to obtain the diffraction patterns of selected samples. The scan step size was 0.02° with a 0.5-s count time over the range $10° < 2\theta < 110°$. The peak data were converted to d spacings, and intensities were manually matched to existing data for possible compounds. Lattice parameters were determined with an indexing routine supplied by Philips. Relative intensities of the major peaks for each compound were used to estimate the amounts of each phase. The high-temperature X-ray equipment has been described previously.[4] For these measurements the sample was rapidly

(1) Cava, R. J.; et al. *Nature* **1988**, *336*, 211.
(2) Subramanian, M. A.; et al., submitted to *Physica B+C (Amsterdam)*.
(3) James, A. C. W. P.; Murphy, D. W. *Chem. Mater.*, this issue.
(4) Gallagher, P.K.; O'Bryan, H. M.; Sunshine, S. A.; Murphy, D. W. *Mater. Res. Bul.* **1987**, *22*, 995.

0897-4756/89/2801-0277$01.50/0

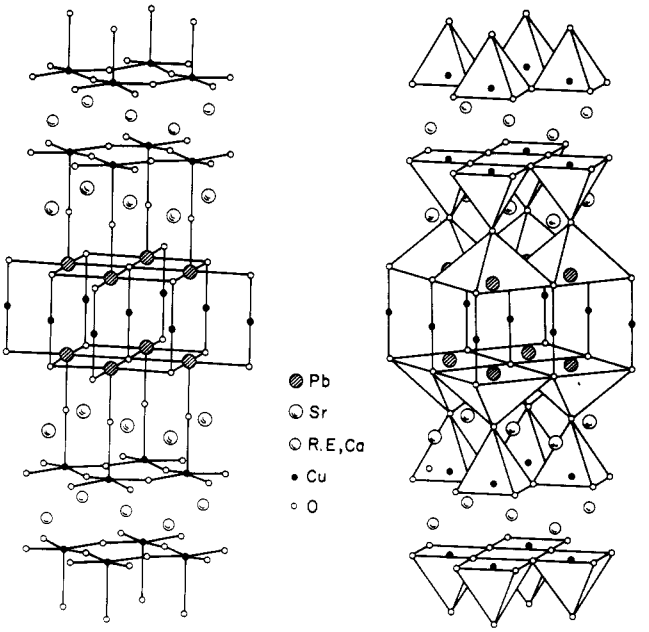

Figure 1. Two representations of the crystal structure for the new superconducting compounds for the case of $Pb_2Sr_2YCu_3O_8$. Left: representation emphasizing the Cu–O and Pb–O bonding scheme. Right: representation emphasizing the manner in which Cu–O and Pb–O polyhedra are arranged.[1]

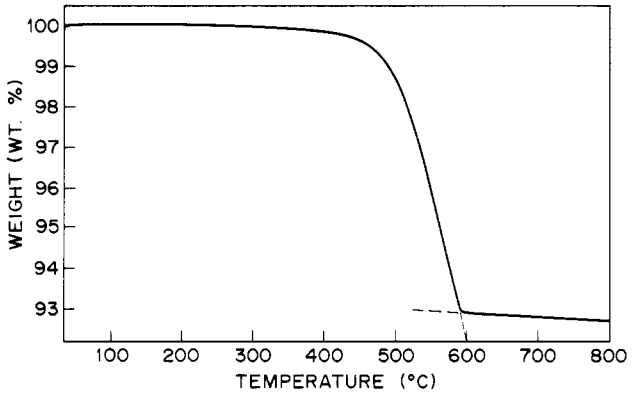

Figure 2. TG curve for $Pb_2Sr_2YCu_3O_{8.00}$ at 10 C min^{-1} in 15% H_2–85% N_2.

heated to temperature in flowing gas (5×10^{-5} atm of O_2 in N_2), and the range $28° < 2\theta < 35°$ was scanned at a 0.01° step size. An upper temperature limit of 800 °C was used in order to minimize contamination of the Pt strip heater, which also served as the sample holder. This is of particular concern at the lower values of P_{O_2}, where Pb is more volatile. The Pt diffraction lines due to the sample holder were used to correct the observed d spacings. When splitting of the (020/200) peaks could no longer be observed, broadening relative to the (114) peak was the indicator that the structure was still orthorhombic. Several X-ray measurements in O_2 at elevated temperatures were made to establish the decomposition temperature of 2213.

Results

Starting Materials. To track quantitatively changes in the oxygen content (δ) as a function of changes in temperature, time, and P_{O_2}, it was necessary to establish accurately an absolute oxygen content for the starting materials. The oxygen content was determined by reduction with H_2 to the rare-earth and alkaline-earth metal oxides plus Cu, Pb, and Ag metals in the manner of earlier work in the $Ba_2YCu_3O_7$ system.[4] Reduction of this phase occurred more readily and without any of the structure in the TG curves so evident in the $Ba_2YCu_3O_7$ system.[5]

Table I. Oxygen Contents and Average Copper[a] Valence

formula	Cu valence[b] Pb^{2+}	Cu valence[b] Pb^{4+}
$Pb_2Sr_2YCu_3O_{8.00}$	1.67	0.33
$Pb_2Sr_2GdCu_3O_{8.01}$	1.67	0.34
$Pb_2Sr_2Y_{0.60}Ca_{0.40}Cu_3O_{8.08}$	1.85	0.52
$Pb_2Sr_2Y_{0.75}Ca_{0.25}Cu_3O_{8.02}$	1.76	0.43
$Pb_2Sr_2YCu_{2.50}Ag_{0.50}O_{8.15}$	1.76	0.43

[a] Or Cu–Ag. [b] Average formal Cu valence based on all of the Pb in the indicated valence state.

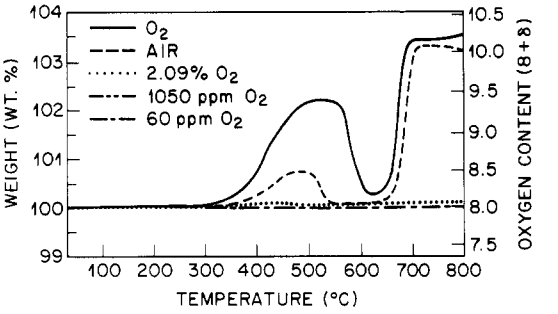

Figure 3. TG curves for $Pb_2Sr_2YCu_3O_{8.00}$ at 2 °C min^{-1} in various atmospheres.

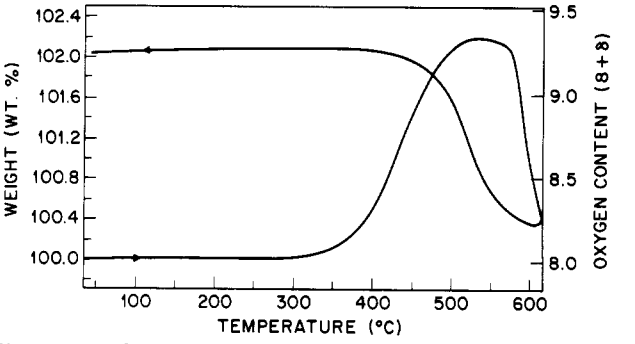

Figure 4. TG curves for $Pb_2Sr_2YCu_3O_{8.00}$ at 2 °C min^{-1} to 600 °C in O_2.

Volatilization of Pb is enhanced by this reducing atmosphere and can be seen above about 600 °C in Figure 2. The completion of reduction was taken as the extrapolated endpoint of the major weight loss as indicated by the dashed lines in Figure 2. A very small correction was made utilizing the appropriate blank experiment. The initial oxygen contents of the samples are presented in Table I along with the calculated average formal valence of Cu based upon the two extremes for the valence of Pb. The values for the unsubstituted compounds are in excellent agreement with the oxygen content proposed in previous work.[1,3] Substitution appears to have led to a small increase in the oxygen content under the synthesis conditions. This apparent excess of oxygen in the substituted materials is unexpected since these substitutions involve a lower valent Ca^{2+} ion for Y^{3+} or a more readily reducible Ag^+ ion for Cu^+. The presence of small amounts of second phases, however, severely affects these calculations. For example, as little as 1.5% of a $SrPbO_3$ phase present in the $Pb_2Sr_2Y_{0.6}Ca_{0.4}Cu_3O_{8.08}$ would lower the true oxygen content of the phase to 8.00. The excess positive charge associated with charge compensation due to the uptake of oxygen is attributed to raising the valence of copper. This is, however, only a "bookkeeping" scheme and does not imply the specific location of this charge.[6]

(5) Gallagher, P. K.; O'Bryan, H. O.; Grader, G. S. *Thermochim. Acta* **1989**, *137*, 343.

Table II. Oxygen Contents and Average Copper Valences[a] at Selected Points for $Pb_2Sr_2YCu_3O_{8.00}$ Heated at 2 °C min^{-1} in the Indicated Atmospheres

O_2				air				2.09% O_2 in N_2				1050 ppm O_2				60 ppm O_2			
T, °C	$8+\delta$	Pb^{2+}	Pb^{4+}	T, °C	$8+\delta$	Pb^{2+}	Pb^{4+}	T, °C	$8+\delta$	Pb^{2+}	Pb^{4+}	T, °C	$8+\delta$	Pb^{2+}	Pb^{4+}	T, °C	$8+\delta$	Pb^{2+}	Pb^{4+}
25	8.00	1.67	0.33	25	8.00	1.67	0.33	25	8.00	1.67	0.33	25	8.00	1.67	0.33	25	8.00	1.67	0.33
522	9.33	2.55	1.22	477	8.42	1.95	0.61	428	8.01	1.67	0.34	861	7.91	1.61	0.28	859	7.86	1.57	0.24
622	8.10	1.73	0.40	589	7.99	1.66	0.33	515	7.98	1.65	0.32	25	7.92	1.61	0.28	25	7.86	1.57	0.24
729	10.08	3.05	1.72	718	10.01	3.00	1.67	684	7.99	1.66	0.32								
849	9.95	2.97	1.63	858	9.57	2.71	1.38	861	7.94	1.62	0.29								
25	10.08	3.05	1.72	25	9.63	2.76	1.42	25	7.95	1.63	0.30								

[a] See footnote *b* in Table I.

Table III. Structure of $Pb_2Sr_2Y_{1-x}Ca_xCu_{3-y}Ag_yO_{8+\delta}$

composition	atmosphere	heating condition	$8+\delta$	phases[c]
$Pb_2Sr_2YCu_3O_{8+\delta}$	60 ppm O_2	slow cooled[a] from 850 °C	7.86	O
	1050 ppm O_2	slow cooled[a] from 850 °C	7.92	O
	2.09% O_2	slow cooled[a] from 850 °C	7.95	O
	air	slow cooled[a] from 850 °C	9.63	P
	O_2	slow cooled[a] from 850 °C	10.08	P + P′
	O_2	slow cooled[a] from 616 °C	9.26	T
	O_2	542 °C/24 h/quenched	9.66	T
	O_2	436 °C quenched	8.31	O
	O_2	509 °C quenched	8.85	O
	O_2	579 °C quenched	8.53	O
	O_2	632 °C quenched	8.08	O
	O_2	683 °C quenched	8.68	O + P
$Pb_2Sr_2GdCu_3O_{8+\delta}$	60 ppm O_2	slow cooled[a] from 850 °C	7.80	O
	O_2	slow cooled[a] from 850 °C	8.01	O
	air	slow cooled[a] from 850 °C	9.66	P
	O_2	slow cooled[a] from 850 °C	9.85	P
$Pb_2Sr_2Y_{0.60}Ca_{0.40}Cu_3O_{8+\delta}$	60 ppm O_2	slow cooled[a] from 850 °C	7.68	O
	1050 ppm O_2	slow cooled[a] from 850 °C	7.83	O
	1.0% O_2	slow cooled[a] from 850 °C	8.08	O + sl P
	2.09% O_2	slow cooled[a] from 850 °C	8.26	O + P
	air	slow cooled[a] from 850 °C	9.83	P
	O_2	slow cooled[a] from 850 °C	9.88	P
$Pb_2Sr_2YCu_{2.50}Ag_{0.50}O_{8+\delta}$	60 ppm O_2	slow cooled[a] from 850 °C	7.51	O + v sl P + Ag
	1.0% O_2	slow cooled[a] from 850 °C	8.15	O + v sl P
	air	slow cooled[a] from 850 °C	9.76	O + sl P
	O_2	slow cooled[a] from 850 °C	9.79	P + P′

[a] 2 °C min^{-1}. [b] Quenched samples were prepared by dropping the TG furnace at selected oxygen contents. [c] O = orthorhombic (2213), P = pseudocubic perovskite, P′ = $SrPbO_3$-like perovskite, T = tetragonal (2213).

$Pb_2Sr_2LnCu_3O_{8+\delta}$. The TG curves at 2 °C min^{-1} for $Pb_2Sr_2YCu_3O_8$ heated in the various atmospheres are shown in Figure 3. The most striking feature is the low-temperature oxidation observed near 400 °C. The material first absorbs O_2 and then at slightly higher temperature loses the absorbed O_2. As expected, the amount of this oxidation diminishes with decreasing P_{O_2}. Reversibility of this low-temperature oxygen uptake is demonstrated in Figure 4, where heating at 2 °C min^{-1} in O_2 was stopped near 600 °C (minimum oxygen content), and the lost weight was almost completely regained during cooling in O_2 at the same rate. Equilibrium is not achieved under normal dynamic heating conditions; the uptake of O_2 for the low-temperature oxidation increases markedly as the heating rate decreases as shown in Figure 5. Because of the kinetic dependence an isothermal experiment was performed at 542 °C in O_2. After about 1000 min the weight approached a constant value, indicating about 1.66 or slightly above is the equilibrium value of δ at that temperature. This is significantly greater than the dynamic value of 1.33 in Figure 3 or 1.32 in Figure 4 for heating at 2 °C min^{-1}. Table II is a summary of the oxygen contents at maxima, minima, and other selected temperatures in different atmospheres. The samples were held for 10 min at the upper temperature prior to cooling at 2 °C min^{-1} to 500 °C and holding for an additional 30 min.

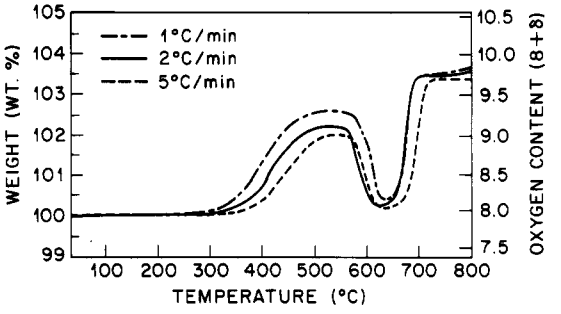

Figure 5. TG curves for $Pb_2Sr_2YCu_3O_{8.00}$ at various heating rates in O_2.

The samples were cooled as rapidly as the furnace would allow from that point.

For samples cooled from 850 °C in 60 ppm, 1050 ppm and 2.09% O_2, only the orthorhombic cell[1] with $a = 5.39$, $b = 5.42$, and $c = 15.72$ Å is observed. The cell sizes are apparently identical with the starting powder ($\delta = 0.00$) in spite of a loss of O_2, which corresponds to as much as $\delta = -0.14$. It must be noted that the values of δ given are all based on the assumption of no Pb volatilization. The loss of very small amounts of Pb at the higher temperatures will have a significant effect, because of its large atomic mass, on the calculated value of δ. In air ($\delta = 1.63$), heating to 850 °C and cooling result in decomposition into a pseudocubic perovskite[2] ($a \approx 8.60$ Å). In O_2 ($\delta = 2.08$) mixed phases, pseudocubic perovskite plus a $SrPbO_3$-like

(6) Sleight, A. *Science* 1988, *242*, 1519.

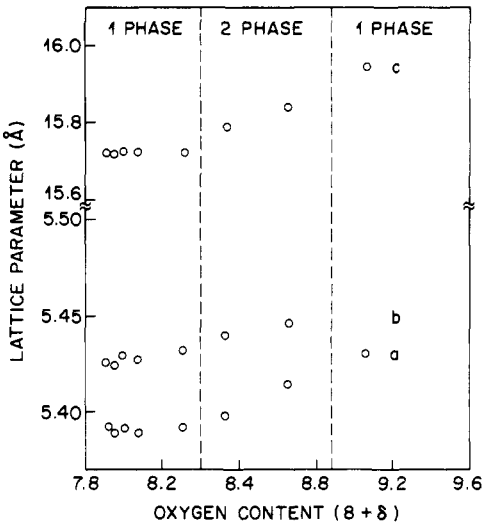

Figure 6. Lattice parameter vs oxygen content for 2213 samples.

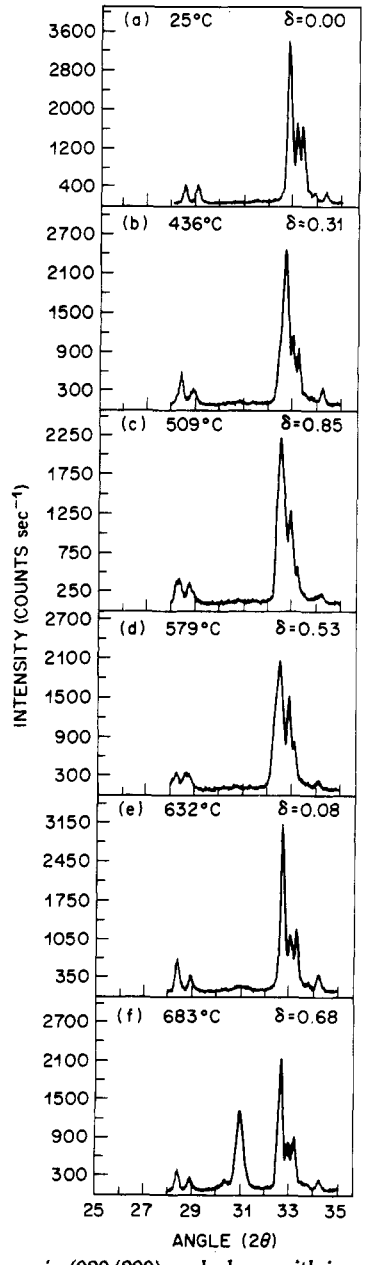

Figure 7. Change in (020/200) peak shape with increasing quench temperature for samples heated in oxygen.

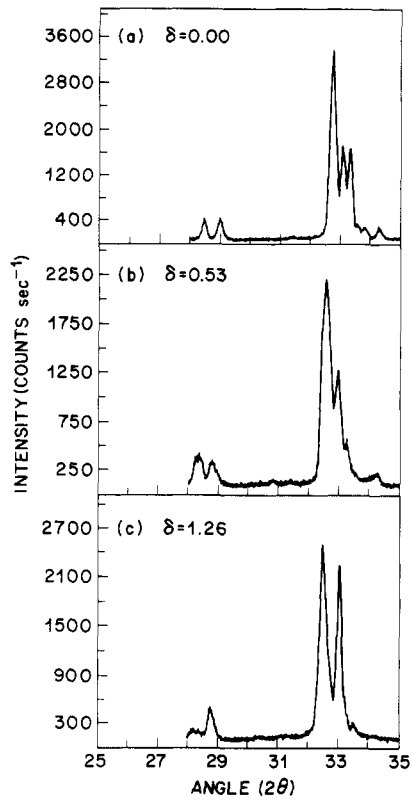

Figure 8. Comparison of peak shapes and intensities for 2213 with varying oxygen contents.

perovskite (a, $b \approx 5.94$ Å, $c = 8.34$ Å), are formed. Table III summarizes the phases detected by X-ray diffraction after various heating conditions.

Lattice parameters for samples heated in O_2 to intermediate temperatures are shown in Figure 6. The change at $\delta = 0.85$ is much greater for the c axis (1%) versus that (~0.1%) for the a and b axes. The assumption of an orthorhombic symmetry phase with a variable, intermediate δ is tentative since the intensity variations for the (020/200) peaks suggest a more complicated situation. Figure 7 shows the $28° \leq 2\theta \leq 35°$ range as the quench temperature in O_2 is increased. The orthorhombic structure should have approximately equal intensities for the (020/200) peaks. Clearly the structure is orthorhombic at $\delta = 0.00$, 0.08, 0.31, and 0.68. For $\delta = 0.85$ and 0.53 (at higher temperature during O_2 loss) the intensities of the (020/200) are no longer equal and it may be conjectured that tetragonal and orthorhombic variants of the same basic structure type coexist. At the highest temperature of 683 °C with $\delta = 0.68$ two phases, a small orthorhombic cell (2213 type) and a pseudocubic perovskite, are noted indicating onset of oxidative decomposition. Figure 8 compares room-temperature X-ray patterns for 2213 having different oxygen contents that were obtained by oxidation followed by a slow cool. These patterns show the evolution of the tetragonal structure as δ increases from 0 to 1.26. Note that no pseudocubic phase has appeared even though the value of δ has reached 1.26.

The weight gain at the higher temperatures in Figure 3 and Table II, e.g., $\delta > 1.7$, is associated with oxidation of the Pb^{2+} and the concomitant decomposition of the 2213 material in the more oxidizing atmospheres. The values of average Cu valence in Table II, therefore, represent the extremes with the actual values dependent on the amount of Pb^{2+} oxidized or the average Pb valence in this decomposition process. Complete oxidation of Pb to 4+ and Cu to 2+ would yield an oxygen content of 10.5, which was

Table IV. Oxygen Contents and Average Copper Valences[a] at Selected Points for $Pb_2Sr_2GdCu_3O_{8.01}$ Heated at 2 °C min^{-1} in the Indicated Atmospheres

O_2				air				60 ppm in N_2			
T, °C	$8+\delta$	Pb^{2+}	Pb^{4+}	T, °C	$8+\delta$	Pb^{2+}	Pb^{4+}	T, °C	$8+\delta$	Pb^{2+}	Pb^{4+}
25	8.01	1.67	0.34	25	8.01	1.67	0.34	25	8.01	1.67	0.34
548	9.58	2.72	1.39	501	8.52	2.01	0.68	384	7.98	1.65	0.32
635	8.35	1.90	0.57	558	8.02	1.68	0.35	563	7.99	1.66	0.33
759	10.19	3.13	1.79	747	10.07	3.05	1.71				
870	9.92	2.95	1.62	871	8.16	1.77	0.44	868	7.85	1.56	0.22
25	9.85	2.90	1.57	25	9.66	2.78	1.44	25	7.80	1.53	0.20

[a] See footnote *b* in Table I.

Table V. Oxygen Contents and Average Copper Valences[a] at Selected Points for $Pb_2Sr_2Y_{0.60}Ca_{0.40}Cu_3O_{8.08}$ Heated at 2 °C min^{-1} in the Indicated Atmospheres

O_2				air				2.09% O_2 in N_2				1050 ppm O_2				60 ppm O_2			
T, °C	$8+\delta$	Pb^{2+}	Pb^{4+}	T, °C	$8+\delta$	Pb^{2+}	Pb^{4+}	T, °C	$8+\delta$	Pb^{2+}	Pb^{4+}	T, °C	$8+\delta$	Pb^{2+}	Pb^{4+}	T, °C	$8+\delta$	Pb^{2+}	Pb^{4+}
25	8.08	1.85	0.52	25	8.08	1.85	0.52	25	8.08	1.85	0.52	25	8.08	1.85	0.52	25	8.08	1.85	0.52
466	9.63	2.88	1.55	495	9.46	2.78	1.44	450	8.21	1.94	0.61	868	7.78	1.66	0.32	865	7.70	1.60	0.27
634	9.04	2.50	1.16	571	8.27	1.98	0.65	509	8.06	1.84	0.51	25	7.83	1.69	0.35	25	7.68	1.59	0.26
697	9.85	3.03	1.70	697	9.82	3.01	1.68	740	9.63	2.89	1.55								
863	9.89	3.06	1.73	864	9.87	3.04	1.71	863	7.91	1.74	0.41								
25	9.88	3.05	1.72	25	9.83	3.02	1.68	25	8.26	1.95	0.62								

[a] See footnote *b* in Table I.

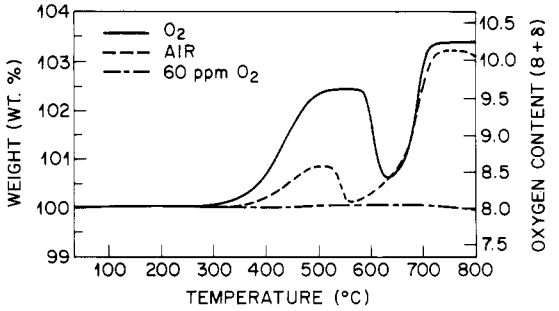

Figure 9. TG curves for $Pb_2Sr_2GdCu_3O_{8.01}$ at 2 °C min^{-1} in various atmospheres.

never achieved in the unsubstituted materials. At higher temperatures, particularly in low P_{O_2}, lead volatilized and the oxygen content also decreased due to reduction of Cu^{2+} to Cu^+ favored at temperatures above about 850 °C.

The TG curves for $Pb_2Sr_2GdCu_3O_{8.01}$ in O_2, air, and N_2 under the same temperature program are shown in Figure 9 and selected values in Table IV. The initial oxidation step continued to a slightly higher temperature and oxygen content, but the substitution of the larger rare-earth-metal ion had little overall effect.

The structure of the Gd material is also orthorhombic for $\delta \leq 0.01$ while its lattice parameters are slightly larger (a = 5.410, b = 5.451, and c = 15.753 Å). Table III shows that a cooling atmosphere of N_2 or 1% O_2 maintains the orthorhombic structure while air or O_2 produces oxidative decomposition and the pseudocubic perovskite phase.

$Pb_2Sr_2(Y,Ca)Cu_3O_{8+\delta}$. The effects of Ca^{2+} substitution for Y^{3+} might be expected to lower the oxygen content by anion vacancy formation as charge compensation. However, as seen in Table I, the opposite effect was observed. Therefore, the charge compensation must occur via oxidation of Cu or Pb. The TG curves of $Pb_2Sr_2Y_{0.60}Ca_{0.40}Cu_3O_{8.08}$ heated in different atmospheres are presented in Figure 10 and Table V. While there are some obvious differences between the behavior of substituted and unsubstituted materials, it is difficult to detect any clear trends in the range of δ. Although the starting oxygen content is slightly greater for the substituted material, it never rises above 10 during the subsequent oxidation and drops to significantly lower values in the less oxidizing atmospheres, e.g., near 7.7 at 865 °C in 60 ppm O_2.

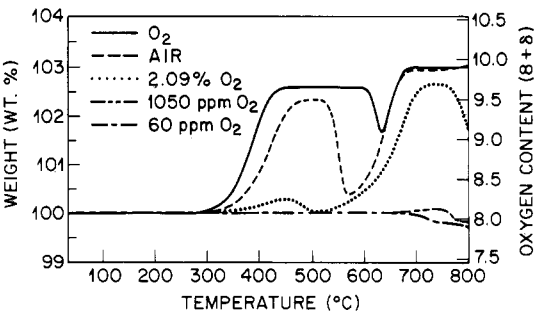

Figure 10. TG curves for $Pb_2Sr_2Y_{0.60}Ca_{0.40}Cu_3O_{8.08}$ at 2 °C min^{-1} in various atmospheres.

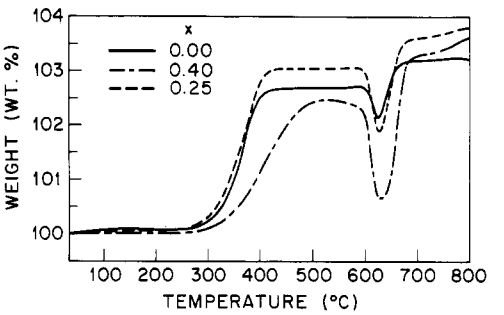

Figure 11. TG curves for $Pb_2Sr_2Y_{1-x}Ca_xCu_3O_{8+\delta}$ at 1 °C min^{-1} in O_2.

Table VI. Oxygen Contents and Average Copper Valences[a] at Selected P_{O_2} in for $Pb_2Sr_2Y_{0.75}Ca_{0.25}Cu_3O_{8.02}$ Heated at 1 °C min^{-1} in O_2

T, °C	$8+\delta$	Pb^{2+}	Pb^{4+}
25	8.02	1.76	0.43
500	9.93	3.03	1.70
620	9.13	2.50	1.17
810	10.39	3.34	2.01
25	10.37	3.33	2.00

[a] See footnote *b* in Table I.

Figure 11 shows TG curves in O_2 at 1 °C min^{-1} for $Pb_2Sr_2Y_{1-x}Ca_xCu_3O_{8+\delta}$ at x = 0, 0.25, 0.40. Because of the changing compositions it is not possible to place a consistent oxygen content scale on the figure. The major point of interest is that the oxygen uptake for both the low- and

Table VII. Oxygen Contents and Average Cu + Ag Valences[a] at Selected Points for $Pb_2Sr_2YCu_{2.5}Ag_{0.5}O_{8.15}$ Heated at 2 °C min^{-1} in the Indicated Atmospheres

O_2				air				60 ppm O_2 in N_2			
T, °C	8 + δ	Pb^{2+}	Pb^{4+}	T, °C	8 + δ	Pb^{2+}	Pb^{4+}	T, °C	8 + δ	Pb^{2+}	Pb^{4+}
25	8.15	1.76	0.43	25	8.15	1.76	0.43	25	8.15	1.76	0.43
533	8.74	2.15	0.82	478	8.25	1.84	0.51	450	8.18	1.78	0.45
621	8.37	1.91	0.58	561	8.20	1.80	0.47	610	8.19	1.79	0.46
816	10.15	3.10	1.77	745	9.84	2.67	1.33	700	8.15	1.76	0.43
900	8.97	2.31	0.98	900	8.15	1.76	0.43	900	7.96	1.63	0.30

[a] See footnote *b* in Table I.

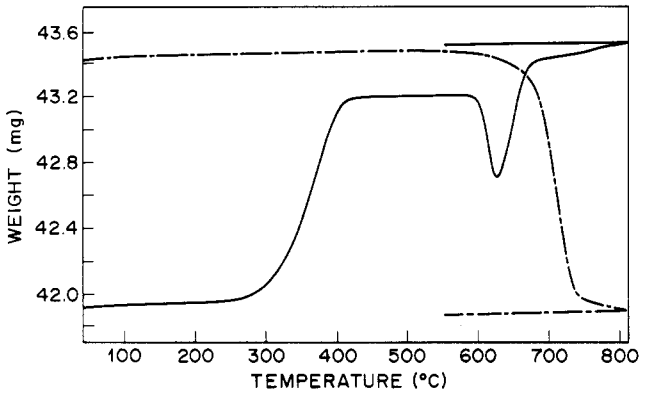

Figure 12. TG curves for $Pb_2Sr_2Y_{0.75}Ca_{0.25}Cu_3O_{8.02}$ at 1 °C min^{-1}, first in O_2 (—) and then reheated in 60 ppm O_2 in N_2 (- - -).

high-temperature peaks goes through a maximum at x = 0.25. The oxygen contents and average Cu valences are given in Table VI for x = 0.25. The oxygen content at the end of the decomposition cycle of 2213 corresponds to all Cu^{2+} and Pb^{4+}. It is interesting to note that the oxygen content at the low-temperature oxidation plateau (~500 °C) corresponds very closely to complete oxidation to Cu^{3+} if Pb remains 2+. Alternatively, if the oxidation is assigned entirely to the formation of Pb^{4+}, then the Cu valence changes very little. It is more likely, however, that the actual situation represents some intermediate condition.

The decomposition process can be reversed as shown in Figure 12 for $Pb_2Sr_2Y_{0.75}Ca_{0.25}Cu_3O_8$. The sample was heated at 1 °C min^{-1} in O_2 to 810 °C and cooled quickly, resulting in mixed O + P phases. When the sample was reheated in N_2 under the same heating program, single-phase orthorhombic 2213 and nearly the original weight were restored.

X-ray diffraction data for the Ca-substituted compound shows the orthorhombic 2213 structure is the major phase obtained by cooling in $P_{O_2} \leq 1\%$. In P_{O_2} = 2.09% appreciable oxidative decomposition to the pseudocubic perovskite is found, and cooling in air and O_2 yield only pseudocubic perovskite (Table III). There is no indication of any $SrPbO_3$-like perovskite phase. The appearance of appreciable perovskite at P_{O_2} = 2.09% indicates that Ca-substituted 2213 is less stable in O_2 then any of the host 2213 compounds. This fact makes the synthesis of single-phase, superconducting, Ca-containing compounds quite difficult, as previously stated.[1]

$Pb_2Sr_2Y(Cu,Ag)_3O_{8+\delta}$. It is of interest to compare the effects of substitution on the Cu sites as well. James and Murphy[3] have shown that Ag substitution takes place on the linearly coordinated Cu^+ sites and give a more detailed description of this particular substitution. Figure 13 shows thermograms of $Pb_2Sr_2YCu_{2.5}Ag_{0.5}O_{8+\delta}$ measured at 2 °C min^{-1} to 900 °C in O_2, air, and 60 ppm O_2. Selected data are listed in Table VII. The thermogram in air resembles that in O_2 below 750 °C, except that very little oxygenation is observed in the 400–600 °C range and oxidative decomposition to metallic Ag and Pb^{4+} perovskite takes place at

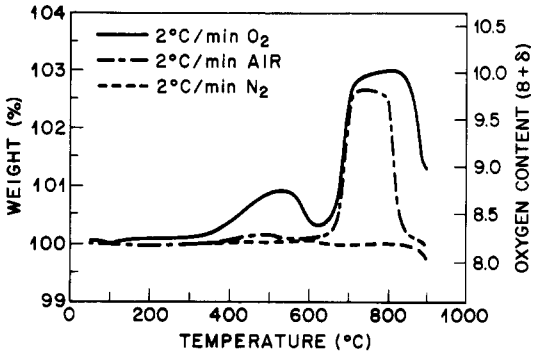

Figure 13. TG curves for $Pb_2Sr_2YCu_{2.50}Ag_{0.50}O_{8.15}$ at 2 °C min^{-1} in various atmospheres.

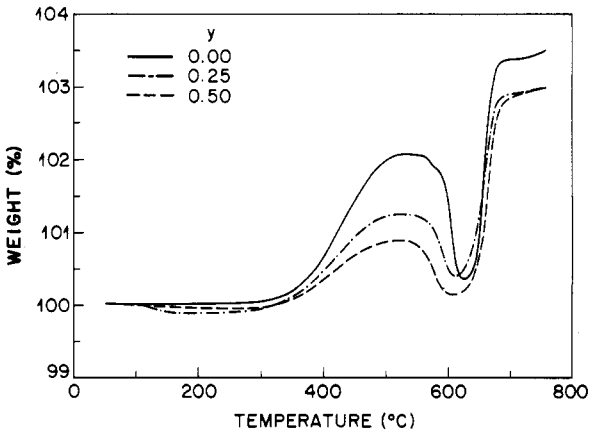

Figure 14. TG curves for $Pb_2Sr_2YCu_{3-y}Ag_yO_{8+\delta}$ at 2 °C min^{-1} in O_2.

a slightly higher temperature than in O_2. The high-temperature oxidation products are themselves unstable and start to decompose back to $Pb_2Sr_2YCu_{2.5}Ag_{0.5}O_8$ above 820 °C. This decomposition goes to completion in air (but not in O_2) at 860 °C. Hence, the best synthesis of $Pb_2Sr_2YCu_{2.5}Ag_{0.5}O_8$ involves heating at 860 °C in air followed by rapid quenching to prevent formation of perovskite on cooling.[3]

The TG of $Pb_2Sr_2YCu_{2.5}Ag_{0.5}O_8$ in N_2 shows no weight change below 800 °C and a small weight loss above 800 °C. This weight loss is due to decomposition of $Pb_2Sr_2YCu_{2.5}Ag_{0.5}O_8$ into metallic Ag, O_2, $Pb_2Sr_2YCu_3O_8$, and other phases.

Figure 14 compares thermograms of $Pb_2Sr_2YCu_{3-x}Ag_xO_{8+\delta}$ with x = 0, 0.25, and 0.50 measured in O_2 at 2 °C min^{-1} from 100 to 750 °C. Clearly, Ag substitution inhibits the reversible oxygenation of the Cu^+ layers in the 400–600 °C region. Like the unsubstituted $Pb_2Sr_2YCu_3O_8$, the amount of oxygen uptake in this temperature range is strongly dependent on the heating rate; the maximum δ values at 541 °C given in Table VII are dynamic, not equilibrium, values. The equilibrium δ for $Pb_2Sr_2YCu_{2.5}Ag_{0.5}O_{8+\delta}$ was determined by heating a sample in O_2 at 500 °C for 60 h. This gave δ_{eq} = 1.0, which value

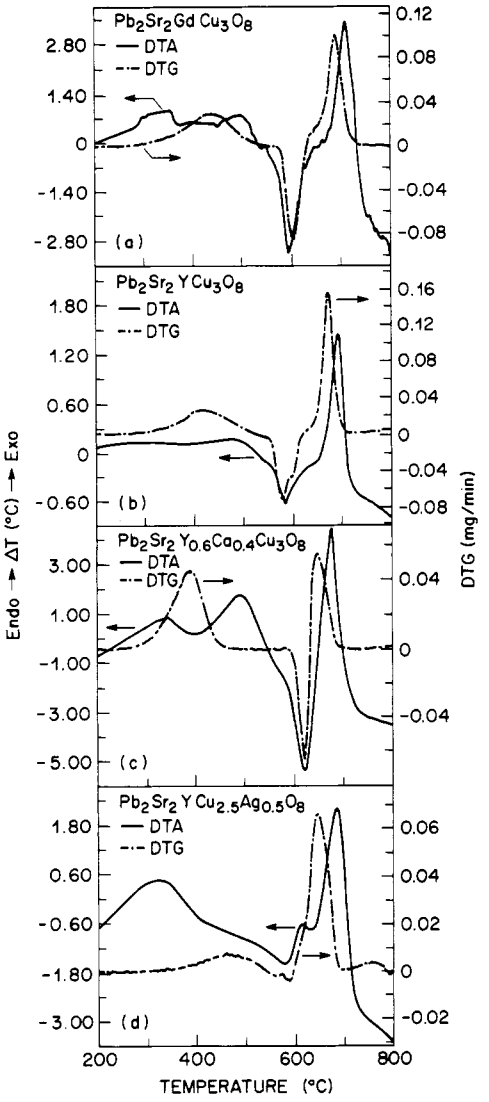

Figure 15. DTA curves at 20 °C min^{-1} and DTG curves at 2 °C min^{-1} in O_2 for various compositions of 2213.

is significantly lower than that for $Pb_2Sr_2YCu_3O_{8+\delta}$ at 542 °C (δ = 1.66). X-ray powder diffraction of the limiting oxygenated composition $Pb_2Sr_2YCu_{2.5}Ag_{0.5}O_{9.0}$ shows that the orthorhombic structure of $Pb_2Sr_2YCu_{2.5}Ag_{0.5}O_{8+\delta}$ is retained with the *a* and *b* lattice parameters unchanged, but that there is a 0.7% expansion of the *c* axis on oxygenation.

Phase Transition

The results of DTA experiments in O_2 are shown in Figure 15 along with the corresponding differential thermogravimetric (DTG) curves. The similarity between the DTA and DTG curves is strong. The qualitative resemblance is overwhelming although there is some displacement in the temperature as a result of the different heating rates, 2 °C min^{-1} for the DTG and 20 °C min^{-1} for the DTA. The low-temperature oxidation is clearly exothermic as would be expected while the subsequent loss of this O_2 is endothermic. The higher temperature oxidation with decomposition is even more strongly exothermic.

The DTA patterns in N_2 naturally show no oxidation; however, there is indication of the higher order phase transition occurring near 750 °C for all materials. The small change in the base line associated with higher order transitions is evident in the DTA curves presented in Figure 16. The high-temperature X-ray data for a N_2

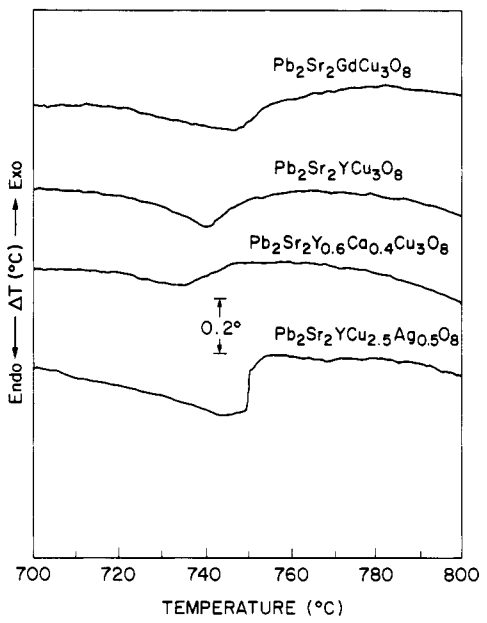

Figure 16. DTA curves at 20 °C min^{-1} in 60 ppm O_2 in N_2 for various compositions of 2213.

atmosphere in Figure 17 also show that a higher order transition to tetragonal symmetry occurs between 700 and 800 °C. Lattice parameters as a function of temperature are presented in Figure 18.

Discussion

The TG data presented above show that a reversible oxidation of the 2213 phase occurs in the temperature range 400–600 °C in air and oxygen. In the parent compound, $Pb_2Sr_2YCu_3O_{8+\delta}$, reversible oxidation in O_2 gives a maximum δ of 1.62 at 542 °C. The orthorhombic parent unit cell has become tetragonal at δ = 1.62. Oxygen is most likely accommodated within the PbO–CuO_δ–PbO plane in the middle of Figure 1. There are two such sites per Cu such that complete occupation would give $Pb_2Sr_2YCu_3O_{10}$. This limiting stoichiometry would make the central Cu octahedral and also increase the oxygen coordination around the Pb. Consequently, a lengthening of the *c* axis would be expected. An increase of 1% in the length of the *c* axis is observed. By contrast, oxygenation of $Ba_2YCu_3O_6$ to $Ba_2YCu_3O_7$ results in a slight decrease in *c* because the central Cu geometry goes from linear, two-coordinate to square planar with much less Cu–O bond lengthening. The failure to reach the limiting stoichiometry implies that at δ = 1.62 both octahedral and square-planar Cu are present in the central plane. One might expect an orthorhombic composition at δ = 1.0 that would contain corner-shared square-planar chains as in $Ba_2YCu_3O_7$, but no plateau indicating uniqueness for that composition was noted.

The oxidation state assignments in the parent compound of $Pb_2^{2+}Sr_2^{2+}Y^{3+}Cu_2^{2+}Cu^{+}O_8^{2-}$ become less clear on addition of oxygen. Up to δ = 1.0 the Cu^+ could be considered as going to Cu^{3+}. Beyond δ = 1.0 either Pb or the five-coordinate Cu must also be oxidized. Alternatively both the Cu^+ and Pb^{2+} could become oxidized for all $\delta > 0$. Aliovalent substitution of Ca^{2+} for Y^{3+} leads to oxidation of the five-coordinate Cu layers and superconductivity, but oxidation with oxygen alone does not lead to superconductivity, suggesting that consideration of the microscopic distribution of charge within the unit cell is critical in determination of the properties.

The reversible oxygen uptake is followed by an irreversible oxidation beginning around 630 °C. This oxida-

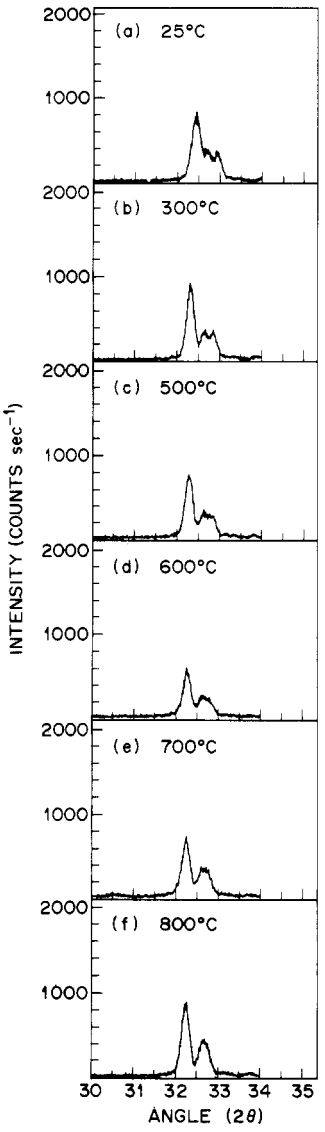

Figure 17. X-ray line profiles for $30° < 2\theta < 34°$ as a function of temperature for $Pb_2Sr_2GdCu_3O_{8.01}$ heated in 60 ppm O_2 in N_2.

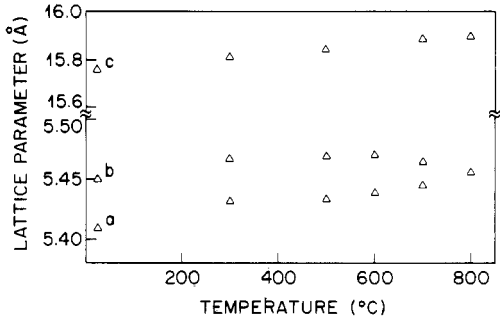

Figure 18. Lattice parameter vs temperature for Gd-2213.

tion results in decomposition of the 2213 to phases clearly containing Pb^{4+}. The smaller size of Pb^{4+} compared to Pb^{2+} leads to stabilization of perovskite-like structures with Pb^{4+} on the small metal atom B sites. Two phases are seen, $Sr_2YCu_2PbO_x$,[2] which is a Pb-substituted analogue of $Ba_2YCu_3O_7$, and an $SrPbO_3$-like perovskite with a tetragonal cell a = 5.94, c = 8.34 Å. When Ag-substituted phases are heated to this temperature, elemental Ag is formed. A reduction back to Pb^{2+} and the 2213 structure does occur above about 850 °C (depending on the P_{O_2}). The 2213 structure, in fact, is best prepared by quenching from above this temperature to prevent Pb^{4+} phases from forming on cooling. Studies of cation-substituted phases as a function of P_{O_2} reveal a balance that must be considered for successful synthesis; as Ca^{2+} substitution for Y^{3+} increases, the maximum P_{O_2} for high-temperature stability decreases. Thus, the greatest level of Ca^{2+} substitution (leading to maximum T_c) is best achieved in 1% oxygen. A similar consideration limits Ag substitution for Cu, and reduced P_{O_2} leads to formation of elemental Ag. One can conclude that the lower oxygen uptake of the silver-substituted materials at 400–600 °C in Figures 13 and 14 is not only a kinetic effect but also reflects a lower thermodynamic limit to the oxygen content in the $Pb_2Sr_2YCu_3O_8$ structure when Ag^+ replaces some of the Cu^+. This conclusion is consistent with the known solid-state chemistry of silver: Ag^{2+} is not a known oxidation state for Ag, and formation of Ag^{3+} requires low temperatures and very highly oxidizing conditions.

Conclusions

The oxygen content of samples of $Pb_2Sr_2Ln_{1-x}M_xCu_{3-y}Ag_yO_{8+\delta}$ can be successfully determined by H_2 reduction, if the cation ratios are accurately known. The upper temperature is limited to about 600 °C where the loss of Pb becomes significant in these reducing atmospheres.

The synthesis conditions used were successful in preparing stoichiometric specimens, i.e., $\delta = 0.00 \pm 0.01$. These conditions, however, apparently resulted in slightly oxidized samples for the materials with partial substitutions, i.e., $Pb_2Sr_2Y_{0.60}Ca_{0.40}Cu_3O_{8.08}$ and $Pb_2Sr_2YCu_{2.50}Ag_{0.50}O_{8.15}$. A lower P_{O_2} is required for their synthesis at the lower temperatures.

All materials underwent a low-temperature oxidation in the region 300–550 °C. The extent of this reaction showed a strong dependence on heating rate, indicating kinetic control in addition to the thermodynamic dependence upon the P_{O_2}. This was followed at slightly higher temperatures by a region of reversible loss of much of this O_2. The 2213 phase was maintained prior to the onset of an oxidative decomposition. The actual extent of this low-temperature oxidation varied with composition. Maximum oxygen contents reached as high as $\delta = 1.93$ for the Ca-substituted material ($x = 0.25$) at 1 °C min^{-1} in O_2 and $\delta = 1.66$ for the specimen of $Pb_2Sr_2YCu_3O_{8.00}$, which was held isothermally at 542 °C for 20 h. The least amount of low-temperature oxidation, $\delta = 0.50$, was observed for the material with 0.50 Ag substitution at this same heating rate and atmosphere. DTA of these materials in O_2 indicated that this low-temperature oxidation was exothermic while the loss of O_2 that followed was endothermic. The DTA curves in N_2 show a higher order phase transition near 750 °C for all of the compositions. Under oxidizing conditions the samples decompose prior to this transformation.

X-ray diffraction results indicate that the structure during this low-temperature oxidation (≤630 °C) remains orthorhombic or orthorhombic + tetragonal until an oxygen content near $\delta = 1.0$, at which point the structure becomes completely tetragonal. The conversion to tetragonal and expansion in the lattice with increasing oxygen content are opposite to the trends observed for the $Ba_2YCu_3O_{7-\delta}$ system with increasing oxygen content.

At temperatures above approximately 600 °C an oxidative decomposition commences. For the materials heated to 860–870 °C at 2 °C min^{-1} only $x = 0.25$ was totally oxidized, i.e., all Pb^{4+} and Cu^{2+}. The original material could be readily restored by a reheat in low P_{O_2}. At the higher values of P_{O_2} it was also possible to regenerate the starting phase and oxygen content by heating to sufficiently high temperatures; however, care must be

taken to minimize loss of Pb. These higher temperatures offer the major synthetic route, provided that the samples are quenched to avoid significant uptake of O_2 or given a low-temperature anneal at a reduced P_{O_2}.

X-ray diffraction of the specimens heated to decomposition, $\geq \sim 630$ °C, indicated that there are two products formed. Initially a pseudocubic perovskite is formed while at the highest oxygen contents a $SrPbO_3$-like perovskite will form. As indicated above at still higher temperatures the oxygen content is reduced and the 2213 material is reformed.

The results presented here indicate that the oxidation–reduction behavior of the $Pb_2Sr_2(Ln,M)(Cu,Ag)_3O_{8+\delta}$ family of compounds is considerably more complex than that of other high-T_c superconductors. This is due in part to the fact that oxidation can occur over a very wide range of oxygen stoichiometry within the basic 2213 structure type and in part to the fact that Pb^{4+}-containing perovskites are more thermodynamically stable than 2213 under oxidizing conditions. Further, the stability of the 2213 phase in various atmospheres is strongly dependent on the nature of the cations in the structure. Unlike the case for other Cu-based superconductors, mildly reducing synthetic conditions are necessary for the production of superconducting material. Oxidative conditions result in multiphase poor-quality superconducting materials. The changes in microscopic structure and physical properties on oxidation within the 2213 phase are of considerable interest and will be the subject of further study. Especially of interest will be the anticipated complex relation between superconducting T_c, Ln^{3+}/M^{2+} content stoichiometry. The present study provides the chemical and phase stability framework on which these subsequent studies must be based.